Integrity Methods Using Carrier Phase

X.-W. Chang and C.C. Paige
McGill University, Montreal, Quebec, Canada
chang@cs.mcgill.ca, paige@cs.mcgill.ca

V. Perepetchai
Orthosoft Ltd., Montreal, Quebec, Canada
Valerio.Perepetchai@orthosoft.ca

BIOGRAPHIES

Dr. Chang is Assistant Professor at McGill University, School of Computer Science. He holds a B.Sc and an M.Sc in Computational Mathematics from Nanjing University, China, and a Ph.D in Computer Science from McGill University. His main research area is scientific computing with particular emphasis on matrix computations and applications. His current interests include GPS positioning and integrity monitoring.

Dr. Paige is Professor Emeritus at McGill University, School of Computer Science. He holds a B.Sc and a B.Eng. (Electrical) from the University of Sydney, Australia, and a Ph.D in Computer Science from the University of London. His main research area is numerical linear algebra and its applications, and one of his interests is efficient and numerically reliable estimation for linear systems.

Mr. Perepetchai is a Research and Development Specialist at Orthosoft Ltd. He holds a M.Sc in Computer Science from McGill University. His main research interests include GPS integrity monitoring and tracking systems.

ABSTRACT

In [2] two carrier phase based models for integrity monitoring are developed, called there the j-step model and the prior information model. The former uses single difference measurements of several consecutive epochs, while the latter combines the single difference measurements of the current epoch and estimates of integer ambiguities and their error covariances of the previous epoch obtained from the positioning algorithm of van Graas and Lee [16].

This paper presents efficient and numerically reliable integrity methods and simulation results based on the above two models and a third model presented in [10], which is the same as the above prior information model but double difference measurements are used. The maximum residual test statistics are used in all these methods. Our simulation results show that for ramp error rates not smaller than $0.1\,m/s$, all three methods perform very well for fault detection and identification, and for a small ramp rate such as $0.01\,m/s$, both single and double difference prior information methods gives less missed detection rates than the j-step method. Our simulations also show the prior information methods give (much) smaller horizontal protection levels than the j-step method. These methods can also detect single or multiple cycle slips and identify a single cycle slip.

1 INTRODUCTION

Receiver Autonomous Integrity Monitoring (RAIM) is a necessary component for Global Positioning System (GPS) aviation applications. Integrity characterizes a navigation system ability to provide timely warning to users when the GPS should not be used for navigation. The basic idea is to use the inconsistency in the measurement data to derive test statistics to detect a fault (or bias, blunder and outlier) and to remove the failed satellite from the navigation solution allowing the aircraft to proceed safely. In addition to the fault detection and identification (or exclusion) functions, a GPS RAIM system is also expected to provide the horizontal protection level (HPL), which is the smallest detectable horizontal position error for a given probability of false alert and a given probability of missed detection. If a position solution can not be guaranteed to be protected within HPL with the given probabilities, then an alarm must be annunciated.

Carrier phase measurements are of interest to the GPS community because the high precision of carrier phase, when compared with code phase, can provide not only high accurate positioning [16] but also an extremely high level of GPS integrity [10, 13].

In [2] two carrier phase based models for integrity monitoring were developed: called the j-step model and the prior information model. The former uses single difference measurements of several consecutive epochs, while the latter combines the single difference measurements of the current epoch and estimates of integer ambiguities and their error covariances of the previous epoch obtained from the positioning algorithm of van Graas and Lee [16]. The main purpose of this paper is to present numerical efficient and reliable integrity methods based on the above two models and a third model presented in [10] (which is the same as the above prior information model except it uses double difference measurements), and to show the effectiveness of the three methods by simulations.

This rest of the paper is organized as follows. Section 2 outlines the j-step single difference model, the single difference prior information model and the double difference prior information models. Section 3 gives the fault detection and identification test statistics and presents efficient and numerically reliable methods to compute the statistics. Section 4 briefly describes the method for calculating the HPL we will use. In Section 5 computer simulation results are displayed to compare the three methods. Finally the conclusions are drawn in Section 6.

Notation used. We work with reals only, and use $\Re^n$ to denote the class of real n-dimensional vectors, and $\Re^{m\times n}$ the class of real $m \times n$ matrices. We use i, j, k, l, m, n to denote indices and dimensions (superscript i will refer to the i-th satellite, subscript k to the k-th epoch). Lower case Greek letters will denote scalars, while lower case Roman letters will denote vectors. Upper case Roman will denote matrices. One exception is that for the integer ambiguity vector, we use N to follow the tradition in the GPS literature. Superscript T will denote transpose. The unit matrix will be denoted by I and its i-th column by e_i, while $e \equiv (1, 1, \ldots, 1)^T$ ($\equiv$ is used to mean 'is defined to be'). I_n will denote the $n \times n$ unit matrix. An orthogonal matrix means a square matrix with orthonormal columns, so $Q^TQ = I = QQ^T$ if Q is orthogonal. We use $\|x\|_2 \equiv \sqrt{x^Tx}$ for vectors. We use $\mathrm{cov}\{u\}$ to denote the covariance matrix of the random vector u. $u \sim \mathcal{N}(\bar{u}, U)$ will mean u is a a normally distributed random vector with mean $\bar{u}$ and covariance U.

2 CARRIER PHASE BASED INTEGRITY MODELS

In this paper we assume the baseline (the distance between the stationary receiver and the roving receiver) is short. Then single differencing (between the two receivers) is supposed to be able to eliminate the atmospheric refraction, the satellite clock errors, and the satellite ephemeris errors. For one epoch with m satellites available, we have the following single difference (SD) equations

$$\begin{aligned} y_k^{SD} &= E_k^{SD}x_k + \lambda N^{SD} + e\beta_k^{SD} + v_k^{SD}, \\ v_k^{SD} &\sim \mathcal{N}(0, \sigma^2 I_m), \end{aligned} \quad (1)$$

where

$y_k^{SD} \in \Re^m$ is the vector of single difference carrier phase measurements in meters at epoch k;

$x_k \in \Re^3$ is the baseline vector in meters pointing from the stationary receiver to the roving receiver.

$E_k^{SD} \in \Re^{m\times 3}$ is the geometry matrix and its i-th row is the unit vector pointing from the middle of the baseline to the i-th satellite;

λ is the wave length of the carrier frequency in meters;

$N^{SD} \in \Re^m$ is the unknown single difference integer ambiguity vector;

β_k^{SD} is the difference between the two receivers' clock biases in meters;

$v_k^{SD} \in \Re^m$ is the single difference noise vector.

Notice (1) is actually a nonlinear equation since the geometry matrix E_k^{SD} depends on the baseline vector x_k. But E_k^{SD} can be approximated by using the estimate $\hat{x}_{k-1}$ of x_{k-1} at the beginning of the computation of the estimate $\hat{x}_k$ and one more iteration can usually get a good approximation of E_k^{SD}. So we will assume E_k^{SD} is known in this paper.

Many positioning algorithms use double differenced (DD) carrier phase measurements. Without loss of generality, we assume the first satellite is a reference satellite and define the $(m-1) \times m$ matrix J and the $(m-1)$-vector y_k^{DD} of double differenced measurements:

$$J \equiv [e, -I_{m-1}], \quad y_k^{DD} \equiv Jy_k^{SD}.$$

Then defining

$$E_k^{DD} \equiv JE_k^{SD}, \quad N^{DD} \equiv JN^{SD}, \quad v_k^{DD} \equiv Jv_k^{SD},$$

we have from (1) the double difference equation

$$\begin{aligned} y_k^{DD} &= E_k^{DD}x_k + \lambda N^{DD} + v_k^{DD}, \\ v_k^{DD} &\sim \mathcal{N}(0, \sigma^2 JJ^T). \end{aligned} \quad (2)$$

Notice the single differenced receiver clock bias β_k^{SD} has been canceled since $Je = 0$. Out integrity models will be based on (1) and (2).

2.1 The j-step single difference model

For one epoch, the number of unknowns in (1) is larger than the number of equations. In order to perform meaningful least squares estimation, we need to accumulate the measurements from a few epochs.

The single difference measurement equations at j epochs $k-j+1, k-j+2, \ldots, k$ give

$$y = Fw + v, \qquad v \sim \mathcal{N}(0, \sigma^2 I_{jm}) \tag{3}$$

where

$$y = \begin{bmatrix} y_k^{SD} \\ y_{k-1}^{SD} \\ \cdot \\ y_{k-j+1}^{SD} \end{bmatrix}, \quad w = \begin{bmatrix} x_k \\ \beta_k^{SD} \\ x_{k-1} \\ \beta_{k-1}^{SD} \\ \cdot \\ x_{k-j+1} \\ \beta_{k-j+1}^{SD} \\ N^{SD} \end{bmatrix}, \quad v = \begin{bmatrix} v_k^{SD} \\ v_{k-1}^{SD} \\ \cdot \\ v_{k-j+1}^{SD} \end{bmatrix},$$

$$F = \begin{bmatrix} E_k^{SD} & e & & & & & \lambda I_m \\ & & E_{k-1}^{SD} & e & & & \lambda I_m \\ & & & & \cdot & & \cdot \\ & & & & E_{k-j+1}^{SD} & e & \lambda I_m \end{bmatrix}.$$

Since the coefficient matrix F does not have full column rank, a transformation of unknowns is needed to overcome this problem. Writing

$$\begin{aligned} s_k &\equiv e\,\beta_k^{SD} + \lambda N^{SD}, \\ \Delta_{i,k} &\equiv \beta_{k-i+1}^{SD} - \beta_k^{SD}, \quad i = 2, 3, \ldots, j, \end{aligned} \tag{4}$$

we have the transformed model from (3):

$$y = Gz + v, \qquad v \sim \mathcal{N}(0, \sigma^2 I_{jm}),$$

where

$$y = \begin{bmatrix} y_k^{SD} \\ y_{k-1}^{SD} \\ \cdot \\ y_{k-j+1}^{SD} \end{bmatrix}, \quad z = \begin{bmatrix} x_k \\ x_{k-1} \\ \Delta_{2,k} \\ \cdot \\ x_{k-j+1} \\ \Delta_{j,k} \\ s_k \end{bmatrix}, \quad v = \begin{bmatrix} v_k^{SD} \\ v_{k-1}^{SD} \\ \cdot \\ v_{k-j+1}^{SD} \end{bmatrix},$$

$$G = \begin{bmatrix} E_k^{SD} & & & & & I_m \\ & E_{k-1}^{SD} & e & & & I_m \\ & & & \cdot & & \cdot \\ & & & E_{k-j+1}^{SD} & e & I_m \end{bmatrix}.$$

The above model was introduced in [2] and was called the j-step model. A similar model for positioning and fault detection was introduced in [6], where single differnce measurements between two satellites were used. The model with a possible fault in the measurement from the i-th satellite, $i \leq m$, at epoch k is then

$$y = Gz + e_i\beta + v, \qquad v \sim \mathcal{N}(0, \sigma^2 I_{jm}) \tag{5}$$

where β is a scalar for a possible fault. Notice the possible fault only appears in one of the first m equations in (5).

For position estimation we require that the number of equations in (5) be great than or equal to the number of unknowns. For fault detection the number of equations should be at least one more than the number of unknowns, and for fault identification, the number of equations should be at least two more than the number of unknowns. For details about the requirements of the number of satellites and the number of epochs, see [2].

The position estimates obtained from (5) are not as good as the estimates obtained from the van Graas and Lee algorithm [16], since the former uses only information from a few epochs and the latter uses all information from all previous epochs and the current epoch. In our integrity tests, the van Graas and Lee algorithm rather than (5) is used for positioning.

2.2 The single difference prior information model

In this and the following subsections we give the integrity testing models which explicitly use the information from a positioning algorithm. Specifically we will use the van Graas and Lee algorithm [16].

When the ambiguity vector is fixed as a vector of integers, it can be regarded as known, and can be moved from the right hand side of (1) to the left hand side. Then code based integrity techniques can be used to handle the carrier phase case, see for example [13]. But if the integer ambiguity vector is not fixed (see for example [16]) or before it is fixed, we should regard it as unknown. Standard carrier phase positioning algorithms can provide not only an estimate of the integer ambiguity vector but also its covariance matrix at each epoch. This information can be used in the next epoch. Since many positioning algorithms estimate the double differenced (DD) integer ambiguities (see for example [16]), we can use the following equations:

$$\begin{cases} y_k^{SD} = E_k^{SD} x_k + \lambda N^{SD} + e\beta_k^{SD} + v_k^{SD}, \\ N_{k-1}^{DD} = N^{DD} + \tilde{N}_{k-1}^{DD}, \end{cases} \tag{6}$$

where the first set of equations is just (1), $N_{k-1}^{DD} \in \Re^{m-1}$ is the estimate of the double differenced integer ambiguity vector N^{DD} at epoch $k-1$ and is available from a positioning algorithm, and $\tilde{N}_{k-1}^{DD}$ is the error in N_{k-1}^{DD}. $\tilde{N}_{k-1}^{DD}$ follows the normal distribution $\mathcal{N}(0, V_{k-1}^{N})$, where the covariance matrix $V_{k-1}^{N} \in \Re^{(m-1)\times(m-1)}$ is obtained from the positioning algorithm.

Using $s_k = e\,\beta_k^{SD} + \lambda N^{SD}$ from (4) and noticing $Je = 0$, we have from (6) that

$$\begin{bmatrix} y_k^{SD} \\ \lambda N_{k-1}^{DD} \end{bmatrix} = \begin{bmatrix} E_k^{SD} & I_m \\ 0 & J \end{bmatrix} \begin{bmatrix} x_k \\ s_k \end{bmatrix} + \begin{bmatrix} v_k^{SD} \\ \lambda \tilde{N}_{k-1}^{DD} \end{bmatrix},$$

or

$$y = G\,z + v, \quad v \sim \mathcal{N}\left(0, \begin{bmatrix} \sigma^2 I_m & 0 \\ 0 & \lambda^2 V_{k-1}^{N} \end{bmatrix}\right).$$

The above model was introduced in [2] and also appears in [10], and was called the single difference prior information model. The model is based on a positioning algorithm. But when y and G are known from a positioning algorithm, we can estimate the baseline x_k again by using this model. We found that the van Grass and Lee algorithm [16] position estimate is almost the same as the new position estimate by this model.

Suppose a fault appears in the i-th satellite at epoch k, then like (5) the model with the possible fault is

$$y = G\,z + e_i\beta + v, \quad v \sim \mathcal{N}\left(0, \begin{bmatrix} \sigma^2 I_m & 0 \\ 0 & \lambda^2 V_{k-1}^{N} \end{bmatrix}\right), \quad (7)$$

where β is a scalar for a possible fault. Notice here the possible fault only appears in one of the first m equations in (7). For the requirements of the number of satellites for fault detection and fault identification, see [2].

2.3 The double difference prior information model

As we pointed out earlier, many carrier phase based positioning algorithms use double differenced measurements, where the receivers' clock biases can be canceled. So it will be natural to use double differenced measurements in the integrity model if it is based on such positioning algorithms. Combining (2) and the second equation in (6) gives

$$\begin{bmatrix} y_k^{DD} \\ N_{k-1}^{DD} \end{bmatrix} = \begin{bmatrix} E_k^{DD} & \lambda I_{m-1} \\ 0 & I_{m-1} \end{bmatrix} \begin{bmatrix} x_k \\ N^{DD} \end{bmatrix} + \begin{bmatrix} v_k \\ \tilde{N}_{k-1}^{DD} \end{bmatrix},$$

or

$$y = G\,z + v, \quad v \sim \mathcal{N}\left(0, \begin{bmatrix} \sigma^2 JJ^T & 0 \\ 0 & V_{k-1}^{N} \end{bmatrix}\right).$$

This model was presented in [10] and can be called the double difference prior information model. The model with a possible fault in the measurement from the $(i+1)$-st satellite at epoch k is then

$$y = G\,z + e_i\,\beta + v, \quad v \sim \mathcal{N}\left(0, \begin{bmatrix} \sigma^2 JJ^T & 0 \\ 0 & V_{k-1}^{N} \end{bmatrix}\right), \quad (8)$$

where β is a scalar for a possible fault. Notice if the possible fault appears in the measurement from the reference satellite (the 1st satellite), then the first $m-1$ equations in (8) all have a fault ($e_0 = [1,\ldots,1,0,\ldots,0]^T$).

3 TEST STATISTICS AND THEIR COMPUTATIONS

Three carrier phase based integrity models have been introduced in the previous section, and they have the following form

$$y = Gz + e_i\beta + v, \quad (9)$$

where we assume G is $n \times p$ and has full column rank. Recall for the (single difference) j-step model (5) and the single difference prior information model (7), the possible fault appears in only one of the first m equations, while in the double difference prior information model (8), the possible fault may appear in all of the first $m-1$ equations if the measurement from the reference satellite has a fault, or in only one of the first $m-1$ equations if the measurement from a non-reference satellite has a fault. For fault detection and identification, we use the following quantities as test statistics (see [15, p.282]):

$$\delta_i \equiv \frac{e_i^T(\mathrm{cov}\{v\})^{-1}\hat{r}}{\sqrt{e_i^T(\mathrm{cov}\{v\})^{-1}\mathrm{cov}\{\hat{r}\}(\mathrm{cov}\{v\})^{-1}e_i}}, \quad (10)$$

where $i = 1,\ldots,m$ for models (5) and (7), and $i = 0,1,\ldots,m-1$ for model (8); $\hat{r}$ is the residual vector for the (generalized) least square estimate of z in (9).

At each epoch, $\max_i |\delta_i|$ is compared with a threshold θ_{fa}. If the former is larger than the latter, we will say that a fault has occurred and identify the corresponding satellite which makes $|\delta_i|$ maximum as faulty.

Notice that if there is no fault in any measurement, i.e. $\beta = 0$, then δ_i follows a standard normal distribution $\mathcal{N}(0,1)$ with density function:

$$\rho(\zeta) = \frac{1}{\sqrt{2\pi}} \exp\left(-\frac{1}{2}\zeta^2\right).$$

Given a false alert probability $\mathcal{P}_{\text{fa}}$, the threshold θ_{fa} can be determined from (see [4]):

$$\begin{aligned}\mathcal{P}_{\text{fa}} &= \mathcal{P}\{\max_i |\delta_i| > \theta_{\text{fa}} \,|\, \beta = 0\} \\ &\approx m\mathcal{P}\{|\delta_i| > \theta_{\text{fa}} \,|\, \beta = 0\} = 2m \int_{\theta_{\text{fa}}}^{\infty} \rho(\zeta) d\zeta.\end{aligned}$$

Note that here our definition of false alert probability is conditioned on zero fault, and it is slightly different from that given in [5].

Now we would like to discuss how to compute the test statistics in an efficient and numerically reliable way. The basic idea is to use orthogonal transformations which can ensure good numerical stability. In designing algorithms, we need to make use of the structure of the problem to make the algorithms efficient. Here there are two different cases:

Case 1: the j-step model (5). Notice for this model $\text{cov}\{v\} = \sigma^2 I$, which makes the computation of δ_i simple. Let the $n \times p$ G have QR factorization, with orthogonal $Q = [Q_1, Q_2]$ and upper triangular R,

$$G = [\underbrace{Q_1}_{p}, \underbrace{Q_2}_{n-p}] \begin{bmatrix} R \\ 0 \end{bmatrix} = Q_1 R. \tag{11}$$

This can be computed by using Householder transformations (see for example [3, Chap 5]). Certainly the sparse structures of G in the model should be used during the computations. Then with the least squares estimate $\hat{z} = (G^T G)^{-1} G^T y = R^{-1} Q_1^T y$, the residual vector satisfies

$$\begin{aligned}&\hat{r} = y - G\hat{z} = (I - Q_1 Q_1^T) y = Q_2 Q_2^T y, \\ &\text{cov}\{\hat{r}\} = \sigma^2 Q_2 Q_2^T.\end{aligned}$$

Thus from (10) we have for the m test statistics

$$\delta_i = \frac{e_i^T \hat{r}}{\sqrt{e_i^T Q_2 Q_2^T e_i}} = \frac{(Q_2^T e_i)^T (Q_2^T y)}{\|Q_2^T e_i\|_2}.$$

Notice in computing δ_i we do not need to compute any inverse.

Case 2: the prior information models (7) and (8). For these two models, $\text{cov}\{v\}$ is not diagonal. Let $\text{cov}\{v\} \equiv V$. Then with the generalized least squares estimate $\hat{z} = (G^T V^{-1} G)^{-1} G^T V^{-1} y$, the residual vector satisfies

$$\hat{r} = y - G\hat{z} = (I - G(G^T V^{-1} G)^{-1} G^T V^{-1}) y, \tag{12}$$
$$\text{cov}\{\hat{r}\} = V - G(G^T V^{-1} G)^{-1} G^T. \tag{13}$$

For efficiency and numerical stability we would like to avoid computing any inverse. In [8], a fast and numerically reliable approach is presented to solve the generalized least square problem. We can use the idea of [8] to develop an efficient and numerically reliable algorithm for computing the test statistics.

Let V have the "reverse" Cholesky factorization

$$V = BB^T, \tag{14}$$

where $B \in \Re^{n \times n}$ is nonsingular upper triangular. Here for efficiency the special structures of V in the two models should be used in the above computation. Then we can use Householder transformations or Givens rotations to find orthogonal matrices $Q = [\underbrace{Q_1}_{p}, \underbrace{Q_2}_{n-p}] \in \Re^{n \times n}$ and $W = [\underbrace{W_1}_{p}, \underbrace{W_2}_{n-p}] \in \Re^{n \times n}$ such that

$$Q^T G = \begin{bmatrix} R \\ 0 \end{bmatrix}, \quad Q_2^T B W = \begin{bmatrix} 0 & S \end{bmatrix}, \tag{15}$$

where $R \in \Re^{p \times p}$ and $S \in \Re^{(n-p)\times(n-p)}$ are upper triangular. Thus

$$Q^T B W = \begin{bmatrix} Q_1^T B W_1 & Q_1^T B W_2 \\ 0 & S \end{bmatrix},$$
$$W^T B^{-1} Q = \begin{bmatrix} (Q_1^T B W_1)^{-1} & -(Q_1^T B W_1)^{-1}(Q_1^T B W_2) S^{-1} \\ 0 & S^{-1} \end{bmatrix}.$$

From these, (14) and (15) it follows that

$$\begin{aligned}&G(G^T V^{-1} G)^{-1} G^T \\ &= Q_1 R \left([R^T, 0] Q^T B^{-T} W W^T B^{-1} Q \begin{bmatrix} R \\ 0 \end{bmatrix} \right)^{-1} R^T Q_1^T \\ &= Q_1 R \left(R^T (Q_1^T B W_1)^{-T} (Q_1^T B W_1)^{-1} R \right)^{-1} R^T Q_1^T \\ &= Q_1 Q_1^T B W_1 W_1^T B^T Q_1 Q_1^T. \\ &= (I - Q_2 Q_2^T) B W_1 W_1^T B^T (I - Q_2 Q_2^T) \\ &= B W_1 W_1^T B^T \quad (\text{since } Q_2^T B W_1 = 0 \text{ from (15)}).\end{aligned}$$

Therefore we have from (10), (12), (13) and (14) that

$$\begin{aligned}\delta_i &= \frac{e_i^T (BB^T)^{-1} (BB^T - BW_1 W_1^T B^T)(BB^T)^{-1} y}{\sqrt{e_i^T (BB^T)^{-1} (BB^T - BW_1 W_1^T B^T)(BB^T)^{-1} e_i}} \\ &= \frac{e_i^T B^{-T} W_2 W_2^T B^{-1} y}{\sqrt{e_i^T B^{-T} W_2 W_2^T B^{-1} e_i}} \\ &= \frac{(W_2^T B^{-1} e_i)^T (W_2^T B^{-1} y)}{\|W_2^T B^{-1} e_i\|_2}.\end{aligned} \tag{16}$$

Let $t \equiv B^{-1} e_i$. Then t can easily be obtained by solving the triangular linear system $Bt = e_i$. In a similar way, $B^{-1} y$ can easily be computed. Then some obvious matrix-vector, vector-vector and scalar-scalar operations will finish the computation of δ_i.

Although the derivation of (16) is lengthy, the computation of δ_i by (16) is efficient and can give more accuracy than a method computing the inverses of matrices if they are ill-conditioned.

4 The METHOD FOR HPL

In addition to the fault detection and identification function, a typical GPS RAIM system is also expected to provide the horizontal protection level (HPL) (and sometimes the vertical protection level (VPL)). The purposes of HPL are to bound any horizontal position error and to screen out bad satellite constellation geometries. Bad geometries are detected and excluded by comparing HPL to the horizontal alert limit (HAL), which is given for a fixed phase of flight. Our HPL computation is based on the approach developed in [4], [7] and [14], and details about this approach can be found in these papers and the references therein.

Since the probability of missed detection $\mathcal{P}_{\mathrm{md}}$ is the joint probability of no-detection $\mathcal{P}_{\mathrm{nd}}$ and a horizontal position error exceeding HPL $\mathcal{P}_{\mathrm{er}}$ (see [5])

$$\mathcal{P}_{\mathrm{md}} = \mathcal{P}_{\mathrm{nd}}\mathcal{P}_{\mathrm{er}}, \tag{17}$$

the HPL can be approximated by (see [4])

$$\mathrm{HPL} = \mathrm{HPL}_{\mathrm{det}}(\mathcal{P}_{\mathrm{nd}}) + \mathrm{HPL}_{\mathrm{stoch}}(\mathcal{P}_{\mathrm{er}}), \tag{18}$$

where $\mathrm{HPL}_{\mathrm{det}}$ and $\mathrm{HPL}_{\mathrm{stoch}}$ are the deterministic and stochastic parts of HPL, respectively.

The deterministic part $\mathrm{HPL}_{\mathrm{det}}$ is obtained by maximizing a horizontal position error due to a fault (bias) over all satellites:

$$\mathrm{HPL}_{\mathrm{det}} = \mathrm{SLOPE}_{\max} \cdot \mathrm{pbias}_{\max}. \tag{19}$$

where $\mathrm{SLOPE}_{\max}$ is a function of the design matrix G and the covariance matrix of v in (9) and $\mathrm{pbias}_{\max}$ is a function of $\mathcal{P}_{\mathrm{nd}}$. For the definitions of these two quantities, see for example [4].

Notice we use the integrity model (9) in computing $\mathrm{HPL}_{\mathrm{det}}$. But the j-step model gives less accurate position estimates than the van Graas and Lee algorithm. In other words, the value of $\mathrm{HPL}_{\mathrm{det}}$ will usually be larger than the true one since we use the van Graas and Lee algorithm for positioning. So it is a conservative approach for the j-step model. But for the two prior information models, we can get a much more precise $\mathrm{HPL}_{\mathrm{det}}$ since the models give almost the same position estimates as the van Graas and Lee algorithm.

The stochastic part $\mathrm{HPL}_{\mathrm{stoch}}$ caused by noise can be approximated by (see [10] and [14])

$$\mathrm{HPL}_{\mathrm{stoch}} = \sqrt{2\zeta_{\max}\ln\left(\frac{1}{\mathcal{P}_{\mathrm{er}}}\right)}, \tag{20}$$

where $\zeta_{\max}$ is the maximum eigenvalue of the covariance matrix of the horizontal position error obtained from the positioning algorithm.

In (17) only $\mathcal{P}_{\mathrm{md}}$ is given and $\mathcal{P}_{\mathrm{nd}}$ and $\mathcal{P}_{\mathrm{er}}$ are unknown. Following [14] and [4], we take $\mathcal{P}_{\mathrm{nd}} = \mathcal{P}_{\mathrm{er}} = 10^{-3}$. and approximate HPL by

$$\mathrm{HPL} = \mathrm{HPL}_{\mathrm{det}}(10^{-3}) + \frac{1}{2}\mathrm{HPL}_{\mathrm{stoch}}(10^{-3}), \tag{21}$$

Notice from (17) $P_{md} = 10^{-6}$. This meets $P_{md} \leq 0.001$, a usual requirement, see for example [5]). Thus this approach gives a quite conservative HPL. For this reason, the factor 1/2 in (21) was introduced, mostly based on simulation experience.

5 COMPUTER SIMULATIONS

5.1 Simulation procedure

In order to see how the RAIM methods introduced in this paper behave, and to compare them, we do computer simulations. All simulations were performed in Matlab on a Dell Dimension 4100 Personal Computer running Windows 2000. A 24 GPS satellite constellation was used in the simulations, and we assumed that 7 satellites were visible at all times. The roving receiver is assumed to be on board an aircraft circling above a reference station at the constant speed of $100\,m/s$. The baseline is about 1 km. The initial vertical position uncertainty is $100\,m$. Each single carrier phase measurement is corrupted by a random normal distributed noise with zero mean and standard deviation $\sigma = 0.001\,m$ (see [16]). A fault is simulated as a ramp error. We take the ramp error rates $0.1\,m/s$ and $0.01\,m/s$ and some ramp error rates larger than $0.1\,m/s$.

The ramp error is introduced in a randomly chosen satellite during each run. The receiver clock offset relative to GPS time is modeled by white noise input to a second order Markov process based on [9].

We also simulated faults as single cycle slips of 1 cycle or 10 cycles, and multiple cycle slips of 1 cycle or 10 cycles. It will be seen that our methods can detect and identify single cycle slips, and can detect multiple cycle slips. As expected, we cannot identify multiple cycle slips.

Monte Carlo simulations repeat a single test procedure a lot of times subject to random noise. The performance of our RAIM methods is investigated in terms of the probability of missed detection. A missed detection takes place when the following two events occur simultaneously (see [5]):

1. a fault goes undetected, meaning that a detection test statistic is less than the threshold θ_{fa};

2. a positioning failure takes place, meaning a position error in the horizontal plane is larger than HPL.

Note the position error is not observable, but we can compute it since the true position is known in our simulations. Each simulation run stops if there is a fault detection, followed by a fault identification, or there is a positioning failure. At each epoch the detection test statistic and the horizontal position error are compared with the detection threshold and HPL, respectively.

The following procedure is used in our simulations [11].

1. Compute the HPL for the given GPS geometry and the test statistics. If the HPL is higher than the HAL, which is taken to be $555\,m$ for the non-precision approach of flight [5], GPS is supposed not to be available for navigation for this kind of flight, and a simulation run stops.
2. Compute the detection threshold $\theta_{\rm fa}$ for a given false alert probability $\mathcal{P}_{\rm fa}$. According to [5], we take $\mathcal{P}_{\rm fa} = 2.76{\cdot}10^{-9}$ (under the assumption that noise source has a correlation time of 1 second).
3. Compute the detection test statistics and the horizontal position error and compare them with the detection threshold $\theta_{\rm fa}$ and HPL, respectively at each epoch.
   (a) If a fault detection occurs, a fault identification is attempted.
   (b) If there is no detection, but a positioning failure takes place, this event is counted as a miss.
4. If either a fault detection or a positioning failure occurs, a simulation run stops.

5.2 Simulation results

Runs	Error	n_{md}^{M1}	n_{wi}^{M1}	n_{md}^{M2}	n_{wi}^{M2}	n_{md}^{M3}	n_{wi}^{M3}
33000	a ramp error, $0.1\,m/s$	0	0	0	0	0	0
33000	a ramp error, $0.01\,m/s$	32684	7	0	1381	0	1598
33000	a cycle slip, $\Delta N = 1$	0	0	0	0	0	0
33000	a cycle slip, $\Delta N = 10$	0	0	0	0	0	0
2000	4 cycle slips, $\Delta N = 1$	0	2000	0	2000	0	2000
2000	4 cycle slips, $\Delta N = 10$	0	2000	0	2000	0	2000

Table 1: Simulation Results.

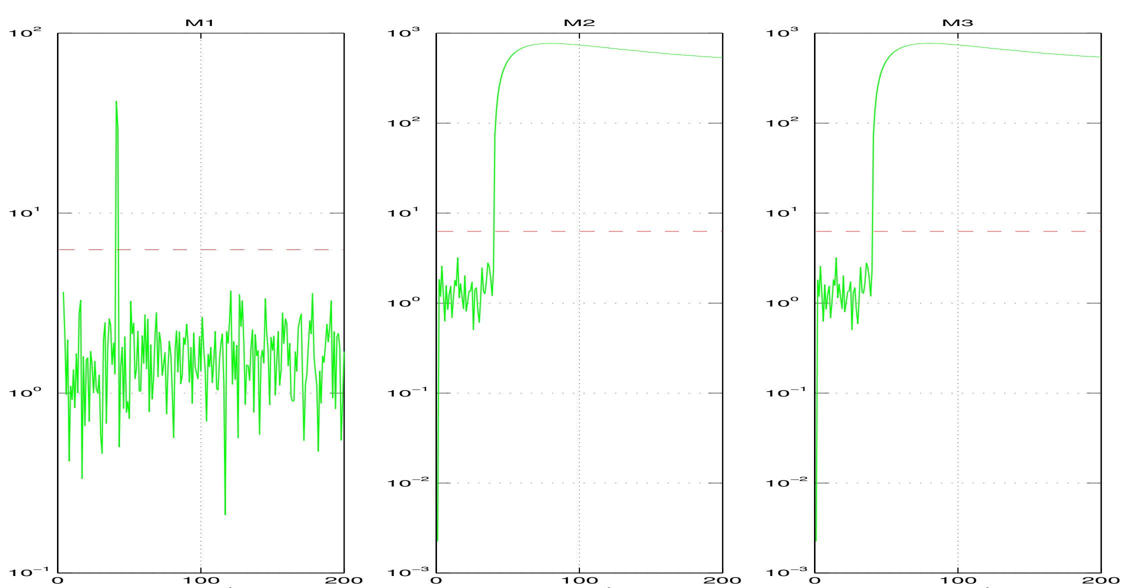

Figure 1: Detection thresholds (dashed lines) and test statistics (solid lines) for the three methods, with a ramp error at a rate of $0.1\,m/s$.

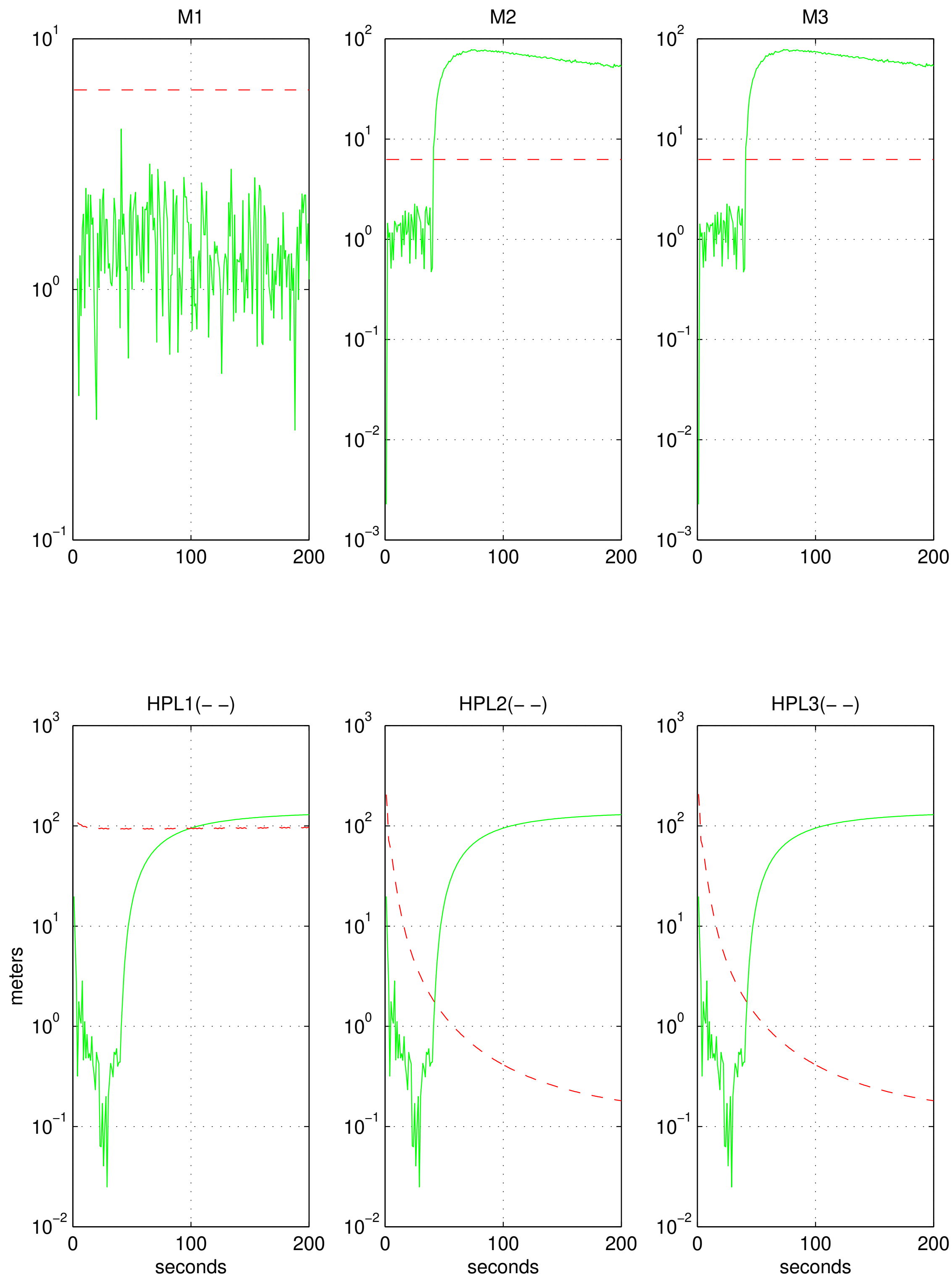

Figure 2: *Top:* Detection thresholds (dashed lines) and test statistics (solid lines). *Bottom:* Horizontal position errors (solid lines) and horizontal protection levels (dashed lines) for the three methods, with a ramp error at a rate of $0.01\,m/s$.

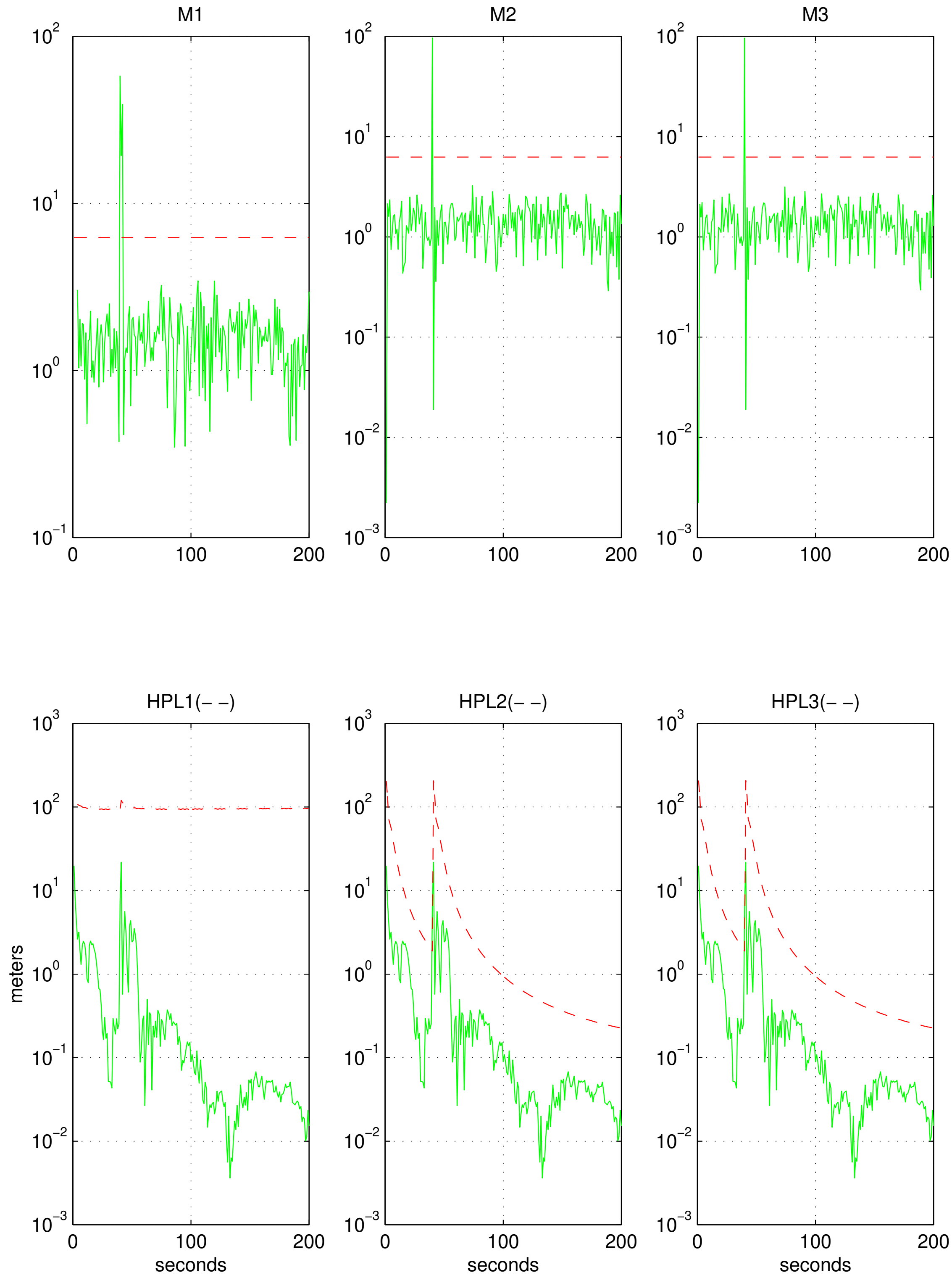

Figure 3: *Top:* Detection thresholds (dashed lines) and test statistics (solid lines); *Below:* Horizontal position errors (solid lines) and horizontal protection levels (dashed lines) for the three method with a single cycle slip $\Delta N = 1$.

We use 7 satellites in all simulations. For the first model, we consider the $j = 4$ case, i.e., the 4-step model. For each model with a ramp error, a test runs 33000 times as suggested in [5]. For the single cycle slip case, a test also runs 33000 times. For the multiple cycle slip case, a test runs 2000 times.

The simulation results are displayed in Table 1, where n_{md} is the number of missed detections, n_{wi} is the number of wrong identifications, and M1, M2 and M3 denote the j-step method, the single difference prior information method and the double difference prior information method, respectively (HPL1, HPL2 and HPL3 in Figures 2 and 3 are the corresponding HPLs by these methods). ΔN denotes the number of cycles slipped in the simulated cycle slip. No false alert occurred in any case with the ramp errors and cycle slips in Table 1.

Table 1 shows that all the RAIM methods detect and correctly identify a ramp error at a rate of $0.1\,m/s$ in 33000 runs. In fact we found from our simulations that it is also true for a ramp error at a rate larger than $0.1\,m/s$. Figure 1 shows the test statistics and thresholds of these methods for the ramp error at the rate of $0.1\,m/s$ for a typical run. The M1 method fails to detect a ramp error of $0.01\,m/s$ in the majority of runs while the M2 and M3 methods detect this error in all runs. The miss is shown in Figure 2 for the M1 method. A ramp error at a rate of $0.01\,m/s$ starts at epoch 40 and goes undetected by the M1 method while its positioning failure occurs at epoch 99. Figure 2 also shows that the M2 and M3 methods detect this ramp error at epoch 41 before a horizontal positioning error caused by this ramp starts exceeding HPL at epoch 43.

From Table 1, we also see for the ramp error at a rate of $0.01\,m/s$, both M2 and M3 methods detect the faults in all runs, but the M2 method performs slightly better than the double difference method. The main difference occurs with satellite 1, the reference satellite in the double difference case. We need to study this further to see if this is due to difference in these two methods or some errors.

We found that the M1 method gives a (much) larger HPL than the M2 and M3 methods, and the HPL for the M1 method does not change much, but the HPLs for the M2 and M3 methods decrease with increasing time, see Figure 2. The reason is that the design matrix G in the j-step model (5) ($j = 4$) is always ill-conditioned, resulting in a large $\mathrm{HPL}_{\mathrm{det}}$, which dominates the HPL and does not change much during the simulation period. In contrast, the design matrices G in the SD prior information model (7) and the DD prior information model (8) are well-conditioned, and with increasing time the covariance matrices of the position error and ambiguity error will decrease, leading to decreases in their HPLs.

For cycle slip errors as shown in Table 1 and displayed in Figure 3, all the three methods detect and correctly identify a single cycle slip (with a slip of 1 cycle, as well as a slip of 10 cycles) in all runs. This is not surprising, since a single cycle slip behaves like a step error when it occurs, and it is always easy to detect and identify a big error. The small jump in HPL1 and big jumps in HPL2 and HPL3 in Figure 3) are due to the cycle slip.

For the multiple cycle slips introduced in 4 of the 7 satellites, all of three methods can detect them, but do not correctly identify them.

6 CONCLUSIONS

We have developed three carrier phase based efficient and numerically reliable methods for integrity tests. Carrier phase measurements are shown to be capable of providing a very high integrity level. As suggested by our simulations, all three methods are able to detect and identify a satellite ramp error of $0.1\,m/s$ and a single cycle slip with the required probability of a missed detection, $P_{md} \leq 0.001$. But for the ramp error at a rate of $0.01\,m/s$, both single and double prior information methods perform much better than the j-step method. They also have a better (lower) HPL then the latter. Therefore we highly recommend the prior information methods for integrity tests.

ACKNOWLEDGEMENTS

This research was supported by NSERC of Canada Grant RGPIN217191-99 and FCAR of Quebec, Canada Grant 2001-NC-66487 for X.-W. Chang, and by NSERC of Canada Grant OGP009236 for C. C. Paige. The authors would like to thank Dr. Boris Pervan, Stanford University, for his helpful comments on navigation requirements and a simulation procedure. This work was finished when the first author was visiting Centre de Recherche en Géomatique of Université Laval, and he would like to thank Dr. Rock Santerre for his hospitality.

References

[1] R. Brown and G. Chin. GPS RAIM: Calculation of Threshold and Protection Radius Using Chi-

Square Methods. *Global Positioning System*, Vol. V, pp. 155–178. The Institute of Navigation, 1997.

[2] X. W. Chang, C. C. Paige, and J. Studenny. Two carrier phase based approaches for autonomous fault detection and exclusion, In *Proceedings of ION GPS-2000*, pp. 1895-1905, Salt Lake City, Utah, September 19-22, 2000.

[3] G. H. Golub and C. F. Van Loan. *Matrix Computations*, 3rd ed. The Johns Hopkins University, Baltimore, 1996.

[4] R. Kelly. The Linear Model, RNP, and the Near-Optimum Fault Detection and Exclusion Algorithm. *Global Positioning System*, Vol. V, pp. 227–259. The Institute of Navigation, 1997.

[5] Y. Lee, K. Van Dyke, B. Decleene, J. Studenny, and M. Bekmann. Summary of RTCA SC-159 GPS Integrity Working Group Activities. *Navigation: Journal of The Institute of Navigation*, 43(3):195–226, 1996.

[6] W. Michakon, H. Hua, and D. Cox. GPS Carrier-Phase RAIM. In *Proceedings of ION GPS-95*, pp. 1995–2004, Palm Springs, CA, September 12-15, 1995.

[7] P. B. Ober. Ways to Improve RAIM/AAIM Availability Using Position Domain Performance Computations. In *Proceedings of ION, the National Technical Meeting*, pp. 485–497, Santa Monica, CA, January 22-24, 1997.

[8] C. C. Paige. Fast Numerically Stable Computations for Generalized Linear Least Squares Problems. *SIAM J. Num. Anal.*, 16:165–171, 1979.

[9] B. W. Parkinson and J. J. Spilker (Eds). *GPS: Theory and Applications*, Vol. 163. Progress in Astronautics and Aeronautics, Washington, DC, 1996.

[10] V. Perepetchai. Global Positioning System Receiver Autonomous Integrity Monitoring. Master's thesis, McGill University, 2000.

[11] B. Pervan. Private communications, 2000.

[12] B. Pervan, C. Cohen, and B. Parkinson. Integrity Monitoring for Precision Approach Using Kinematic GPS and a Ground-Based Pseudolite. *Navigation: Journal of The Institute of Navigation*, 41(2):159–174, 1994.

[13] B. Pervan, D. Lawrence, C. Cohen, and B. Parkinson. Parity Space Method for Autonomous Fault Detection and Exclusion using GPS Carrier Phase. In *Proceedings of PLAN'96 Symposium*, pp. 649–656, Ahanta, CA, April 22-26, 1996.

[14] S. Y. Ryan, G. A. McGraw, and B. T. Driscoll. Investigation and Comparison of Horizontal Uncertainty Protection Level in FDE Algorithms. In *Proceedings of ION GPS-96*, pp. 1607–1621, Kansas City, MO, September 16-19, 1996.

[15] P. J. Teunissen and A. Kleusberg (Eds). *GPS for Geodesy*, 2nd ed. Springer, Berlin, 1998.

[16] F. van Graas and S. Lee. High-Accuracy Differential Positioning for Satellite-Based Systems Without Using Code-Phase Measurements. *Navigation: Journal of The Institute of Navigation*, 42(4):605–618, 1995.